

# Handling of the Tropospheric Delay in Kinematic Precise Point Positioning

N. S. Kjørsvik, *TerraTec A/S, Norway*

J.G.O. Gjevestad and O. Øvstedal, *Norwegian University of Life Sciences, Norway*

## BIOGRAPHY

Dr. Narve Schipper Kjørsvik received his Ph.D. from the Norwegian University of Life Sciences in 2005. He is currently responsible for development of *TerraPos*, a software for kinematic and static Precise Point Positioning made by TerraTec A/S.

Dr. Jon Glenn Omholt Gjevestad received his Ph.D. in telecommunications at the Norwegian University of Science and Technology in 2002. His research interests include satellite radio navigation systems (GNSS), ambiguity resolution and signal processing. He is an Associate Professor of geodesy.

Dr. Ola Øvstedal received his Ph.D. from the Norwegian University of Life Sciences in 2001. He is an Associate Professor of geodesy and land surveying. Research interests include RTK, Precise Point Positioning and ionospheric and tropospheric modeling.

## ABSTRACT

The GPS Standard Positioning Service (SPS) gives a horizontal accuracy of approximately 3–5 m (95%). When operating in differential mode, a number of error sources are mitigated and positional accuracy ranging from a few meters to sub-centimeters can be achieved. In recent years precise satellite ephemerides, satellite clock corrections and earth orientation parameters have become freely available from the International GNSS Service (IGS). For a number of applications the approach of Precise Point Positioning (PPP) has become a viable alternative to differential methods.

In PPP dual frequency code and carrier phase observations from a single GPS receiver are used to estimate receiver coordinates and receiver clock errors as well as a few extra nuisance parameters. In undifferenced GPS observations, the presence of remaining hardware biases makes identification of the integer carrier phase ambiguities difficult. Hence, in PPP processing the carrier phase ambiguities are estimated as real numbers.

Tropospheric errors are usually handled using (i) corrections from a standard model fed with a priori meteorological parameters, (ii) corrections from a standard model fed with meteorological observations or (iii) by estimating the

effect together with other parameters. A priori meteorological parameters may be of inferior quality and reliable meteorological observations may be unavailable. Troposphere parameters will be highly correlated with other parameters when estimated using short observation spans leading to degraded accuracy and a less resistance against outliers and bad observations. The question then raised is how to best handle the tropospheric delay in different PPP applications.

This paper presents a discussion on how to handle tropospheric delay in kinematic PPP processing, some results from kinematic processing of real test data using different processing strategies and some preliminary recommendations.

## INTRODUCTION

Precise Point Positioning (PPP) in kinematic mode is a logistically convenient and efficient method compared to differential methods. Although being a relatively new technique, it is already a preferred method by companies and agencies carrying out e.g. hydrographic surveying and positioning of airborne sensors.

In PPP there is no need for a differential infrastructure in the form of data from regional or local reference receivers, as observations from a single receiver are used.

For GPS the starting point for PPP is the model used in the Standard Positioning Service (ICD-GPS-200c, 2000), used in e.g. handheld GPS receivers, where positions can be estimated with an accuracy of approximately 3–5 m (95%). The most significant feature of PPP is the replacement of the satellite coordinates and satellite clock corrections being broadcasted by the GPS satellites with more accurate products from e.g. the IGS (Beutler *et al.*, 1999). Further refinements in kinematic PPP include using dual frequency code and carrier phase observations, taking into account satellite dependent effects (phase wind up and antenna offsets) and site dependent loading effects (solid earth tide and ocean loading) as well as applying precise earth orientation parameters, see e.g. Kouba and Heroux (2001). The models used in PPP should be compatible to the models used by the agencies supplying satellite coordinates, satellite clock corrections and earth rotation parameters. Using IGS products, IGS and IERS (International Earth Rotation and Reference Systems Service) conventions are to be employed.

In the SPS model, unknown parameters are receiver coordinates and receiver clock errors. In PPP the mathematical model is extended to include carrier phase ambiguities, and for high precision applications also parameters for residual tropospheric delay. The addition of nuisance parameters will in general weaken the geometrical strength of the adjustment.

While the ambiguity parameters have to be included in the model, the residual tropospheric delay parameters can be omitted if the a priori correction model is sufficiently accurate. The handling of tropospheric delay in kinematic PPP by empirical correction models only can generally give a positional accuracy of approximately 0.10 m RMS (Jensen and Øvstedal, 2006). Due to the lack of accurate measurements of temperature, pressure and humidity either a standard atmosphere or a look-up table as function of e.g. time of year, latitude and elevation (e.g. the UNB3 model in Collins and Langley, 1997) are used. Due to local variations of the troposphere, the deviation from standard atmospheric parameters might be significant. If kinematic PPP shall provide 3D coordinates with a consistent accuracy better than some decimeters, residual tropospheric parameters have to be estimated in the adjustment process.

The main focus in the present paper is an attempt to quantify the benefits in terms of reduction of unmodeled tropospheric delay and costs in terms of reduction in geometrical strength of the adjustment associated with estimating residual tropospheric delay parameters. Factors affecting geometrical strength are in this study assumed to be time span of continuous carrier phase observations, elevation cut-off angle and the weighting model of the observations (stochastic model).

After a short discussion of tropospheric delay, results from an empirical test is used to draw some preliminary conclusions.

## TROPOSPHERIC DELAY

An electromagnetic signal penetrating the neutral atmosphere will decrease its velocity due to constituent gases. In addition, refraction will tend to bend the signal path and therefore make it slightly longer. The sum of these two effects are often denoted as "tropospheric delay".

The residual tropospheric range delay due to an incompletely modeled troposphere can usually be ignored by the average user of differential GPS. However, with recent high precision undifferenced processing techniques the unmodeled tropospheric range delay will affect the solution with full impact and therefore must be addressed properly. In general there are two ways of dealing with the tropospheric range delay; one can choose to estimate the effect or one can choose to model the effect.

Normally one assumes the atmosphere to be both horizontally stratified and azimuthally symmetric. With this assumption one usually models the total tropospheric delay as the delay experienced in zenith direction together with a mapping function that scales the zenith delay into the current elevation angle of each satellite. Note that the above assumptions will neglect the existence of any gradients in the

atmosphere. Ignoring these gradients may introduce range errors at the decimeter level at low elevation angles.

The equation for the total tropospheric delay reads:

$$T = T_{hyd}^{ZD} \cdot m_{hyd} + T_{wet}^{ZD} \cdot m_{wet}. \quad (1)$$

$T_{hyd}^{ZD}$  represents the hydrostatic delay which is dependent on the surface pressure only. Under ideal conditions this component can be estimated at the millimeter level.  $T_{wet}^{ZD}$  represents the wet delay which is dependent on the distribution of water vapor in the atmosphere. The only way to measure the wet delay directly is through water vapor radiometers. These kinds of instruments are seldom available.  $m_{hyd}$  and  $m_{wet}$  are functions that scale the hydrostatic and wet zenith delays to corresponding slant delays.

### Tropospheric Delay Models

There exist a number of empirical tropospheric models that can be used to estimate the tropospheric delay with L-band signals (e.g. Saastamoinen, 1973; Hopfield, 1971). The way these models handle the atmospheric input parameters may be divided into two main categories: The first approach is to predict the tropospheric delay from real-time measurements of temperature, pressure and water vapor pressure, and the second approach is to provide these parameters from look-up tables based on time and latitude (e.g. the UNB3 model in Collins and Langley, 1997). However, even with real-time measurements of these input parameters one can not expect to model the tropospheric delay with an accuracy better than a few percent. The reason for this is the highly variable nature of the water vapor pressure that makes the zenith wet delay very hard to predict through models.

### Tropospheric Estimation

The residual tropospheric delay is the remaining part of the tropospheric delay not predicted by empirical models. For high accuracy applications, the residual tropospheric delay can easily be the largest remaining error source. Note that the main disadvantage of estimating the tropospheric delay is the fact that estimating additional parameters in the general minimum variance solution will weaken the system in a geometrical sense, thus affecting other estimated parameters.

Estimating the residual tropospheric delay over short time-spans is in general difficult due to the strong mathematical correlation between the partial derivatives of the tropospheric delay and height (Figure 1). Therefore, one will in general need to accumulate some geometric information in the system to be able to separate the tropospheric delay from other observation errors dependent on direction to each satellite. The impact of the satellite geometry is crucial when estimating tropospheric delay parameters. For short time-spans there must exist observations for low elevation angles (down to approximately 5 degrees) for the estimate of the residual tropospheric delay to be sufficiently accurate. Note that the parameters representing carrier phase biases and the clock errors will absorb some of the residual tropospheric delay.

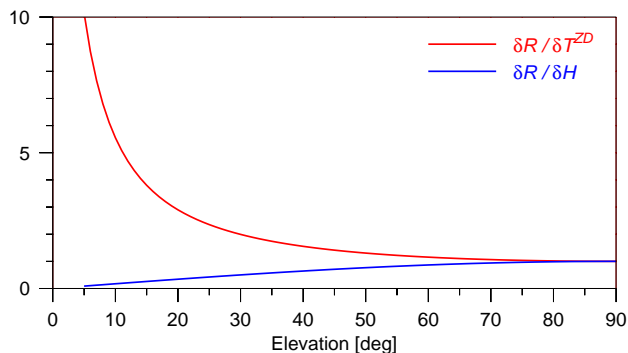


**Fig. 1.** Partial derivatives of the observed range with respect to tropospheric zenith delay and station height respectively.

## TEST DATA AND REFERENCE TRAJECTORY

During spring 2006 the Norwegian Hydrographic Service made a full scale test of their newly acquired PPP software TerraPos from TerraTec. The test included one Topcon Legacy GNSS receiver on a shuttle ferry traveling between Lauvvik and Oanes outside Stavanger, Norway (see Figures 2–3). An identical receiver serving as reference station was deployed close to Lauvvik. Both stations were equipped with identical geodetic antennas. More than 40 days of continuous observations at 1Hz was collected during March–May. Real-Time Kinematic (RTK) solutions were recorded along with raw data.

The raw data were post-processed in differential mode using Geogenius version 2.11 from Spectra Precision Terrasat in 24 hour batches. The post-processed solutions were then compared to the RTK solutions. At each epoch, the average of the two solutions were accepted if the 3D discrepancy was less than 2 cm. The average solutions constitute the reference trajectory. Solutions with floating carrier phase ambiguities were discarded.

## ANALYSIS STRATEGY

### Software

All PPP processing have been done using the *TerraPos* software by TerraTec. This is a state-of-the-art implementation of static and kinematic PPP. Optimal estimation is ensured by using a Kalman filter/smoothen combination (see e.g. Gelb, 1974). Corrections for Earth tides, ocean loading and deformations due to polar motion are applied according to IERS conventions 2003 (McCarthy and Pétit, 2004).

Satellite antenna offsets were taken from the official IGS antenna calibration file. Antenna calibrations for the receiver antennas were taken from the National Geodetic Surveys's database (Mader, 1999), causing all estimated positions to refer to the antenna reference point (ARP).

For marine applications a position/velocity (PV) model is used. The velocities, as well as receiver clock bias and drift are approximated by random walk processes. When estimating residual tropospheric zenith delay, it is also approximated by a random walk process. The hydrostatic mapping function of Niell (1996) is used as partial. Phase

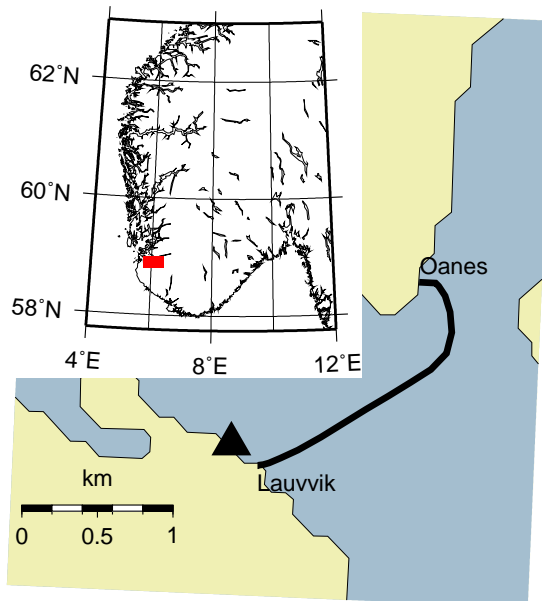


**Fig. 2.** Map showing the test area in south-western Norway. The ferry shuttles along the solid black line. The reference station used to compute the reference trajectory is shown with a triangle.



**Fig. 3.** The shuttle ferry carrying the GPS receiver. The location of the antenna is marked with a red circle.

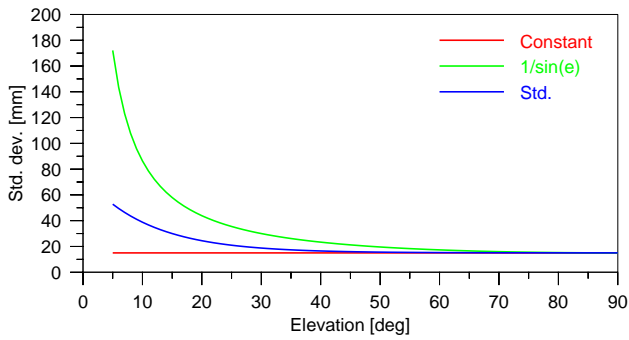


Fig. 4. Functions that map the a priori precision of the phase observations as functions of satellite elevation.

biases are estimated as constants.

No attempts are made to repair cycle slips. A detection causes the associated phase bias parameter to be reset.

The a priori precision of the observations can be modeled as a function of satellite elevation. Three models are currently available; the standard model of TerraPos, a constant model, and the reciprocal sine of elevation. A plot of these weighting functions is shown in Figure 4.

### Processing

Table 1 shows the process noise parameters used in the processing.

Table 1. Spectral amplitudes of the white-noise driving functions for some parameters.

| Process                   | Amplitude                      |
|---------------------------|--------------------------------|
| Along-track velocity      | $4 \text{ m}^2/\text{s}^3$     |
| Cross-track velocity      | $4 \text{ m}^2/\text{s}^3$     |
| Vertical velocity         | $4 \text{ m}^2/\text{s}^3$     |
| Receiver clock bias       | $1.0 \cdot 10^{-8} \text{ s}$  |
| Receiver clock drift      | $4.0 \cdot 10^{-16}/\text{s}$  |
| Tropospheric zenith delay | $0.005^2 \text{ m}^2/\text{h}$ |

Table 2 shows the a priori precision of the observables used in the processing

Table 2. A priori precision of the observables. In case an elevation dependent weighting function is used, the values below are valid for a satellite in zenith direction.

| Observable                       | Standard deviation |
|----------------------------------|--------------------|
| Carrier phase ionosphere free LC | 0.015 m            |
| Code phase ionosphere free LC    | 3.000 m            |

Table 3 shows the initial variance of the parameters. Together, Tables 1–3 define the input parameters to the Kalman filter.

Final precise ephemeris, 30 second satellite clock corrections and earth rotation parameters from Center of Orbit Determination in Europe (CODE) were used throughout this study. Ocean loading coefficients from the GOT00.2 model were downloaded from the automated service at Onsala Space Observatory.

Table 3. Initial variances of some parameters.

| Process                   | Amplitude                     |
|---------------------------|-------------------------------|
| Position                  | $5^2 \text{ m}^2$             |
| Velocity                  | $5^2 \text{ m}^2/\text{s}^2$  |
| Receiver clock bias       | $3.3 \cdot 10^{-7} \text{ s}$ |
| Receiver clock drift      | $1.1 \cdot 10^{-11}$          |
| Tropospheric zenith delay | $0.200^2 \text{ m}^2$         |
| Phase biases              | $10^2 \text{ m}^2$            |

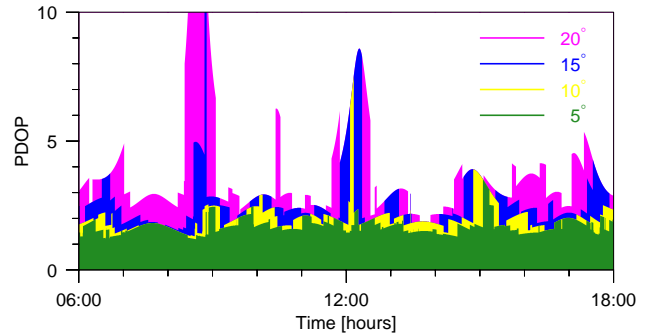


Fig. 5. PDOP using different elevation cutoff angles. Peak values (outside plot range) reach approx. 14 for 15° cutoff and approx. 23 for 20° cutoff.

A priori tropospheric zenith delay is computed using the UNB3 model (Collins and Langley, 1997). Using 10 years of radiosonde data Collins and Langley (1998) found this model to be accurate to 5 cm (one sigma) for North American sites.

Using three different stochastic models for observation precision, elevation cutoff angles of 5°, 10°, 15° and 20°, with and without estimation of residual tropospheric zenith delay, this gives a total of 24 combinations.

12 hours of 1 Hz GPS data (06:00–18:00, April 8th, 2006) were divided into batches of 15 min, 20 min, 30 min, 45 min, 60 min and 120 min. All batches were processed using the 24 strategies, totaling to 3408 runs. The satellite constellation repeats every approx. 12 hours. Hence, effects due to satellite geometry will be attenuated by computing overall statistics for the entire 12 hours data set. A plot of the PDOP is shown in Figure 5.

The reference trajectory was made available in Euref89, the Norwegian realization of the European Terrestrial Reference System (ETRS89) (Kristiansen and Harrison, 1996). Prior to further analysis, the estimated positions from TerraPos were transformed from IGB00 (implied by the ephemeris) to Euref89 using an official transformation provided by the Norwegian Geodetic Institute.

Position errors were computed using the reference trajectory, and overall RMS of the position errors were computed for each batch length and strategy.

## RESULTS

Figure 6 shows coordinate errors for a sequential processing using the a priori tropospheric model only and with estimation of residual tropospheric delay respectively. In these processings no subsequent smoothing is carried out. To improve resolution in the plot, only the first 3 hours are dis-

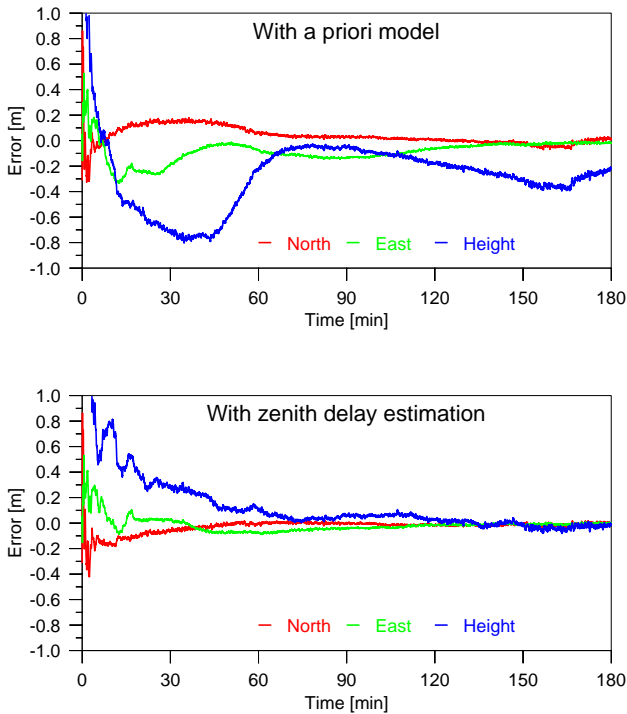


**Fig. 6.** Position errors with a priori troposphere model only (*top*) and with estimation of residual zenith delay (*bottom*). Both plots show the filter solution (no smoothing applied) using the standard stochastic model and  $10^\circ$  elevation cutoff angle.

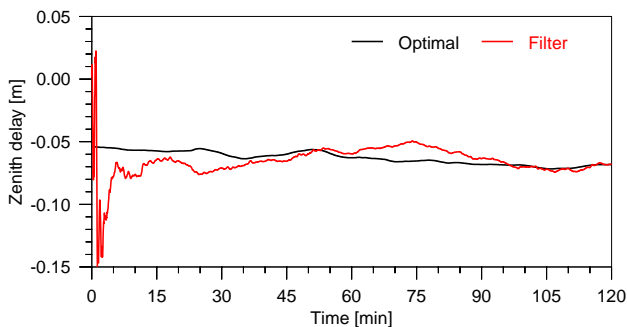


**Fig. 7.** Estimated residual tropospheric zenith delay. Both solutions are computed using the standard stochastic model and  $5^\circ$  elevation cutoff angle.

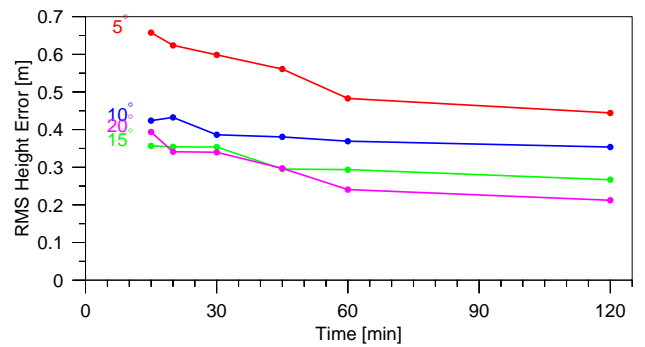


**Fig. 8.** RMS of height errors for varying batch lengths, using the a priori troposphere model only and a constant constant weighting function.

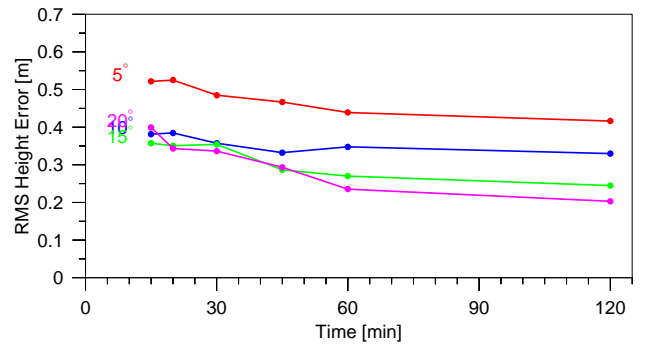


**Fig. 9.** RMS of height errors for varying batch lengths, using the a priori troposphere model only and the standard weighting function.

played.

It can be seen that during the first minutes the accuracy is rather poor. Depending on the a priori model only there is in this data set obvious remaining systematic errors affecting especially the height component. In the case where residual tropospheric delay is estimated, the accuracy during the very first minutes appears to be somewhat worse than in the case using a priori model only, but the accuracy quickly and consistently improves with time.

Figure 7 shows time series of the estimated residual tropospheric delay for the first 2 hours of data from both a sequential processing and a smoothed solution. The residual zenith delay of approximately  $-0.05$  m is well within the expected accuracy of the UNB3 model (Collins and Langley, 1998) but is the obvious reason for the biasedness in Figure 6 – top plot. In the sequential solution, the estimate of the zenith delay parameter only needs a few minutes of continuous observations to become fairly accurate.

Figures 8–13 present results in the form of overall RMS values for each strategy and batch length. In the following we present results for the height component only. Similar results are obtained for the horizontal components. However, the satellite geometry is more unfavorable for precise height determination, and this effect is even more pronounced at high latitudes. In addition, the height component is more sensitive to tropospheric errors due to high correlation with troposphere parameters.

Figures 8–10 show results where the processing depends on the a priori model only while Figures 11–13 show results where residual tropospheric zenith delay is estimated in

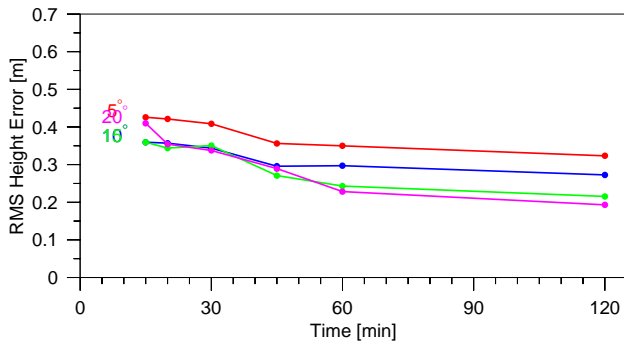


Fig. 10. RMS of height errors for varying batch lengths, using the a priori troposphere model only and the reciprocal of sine as weighting function.

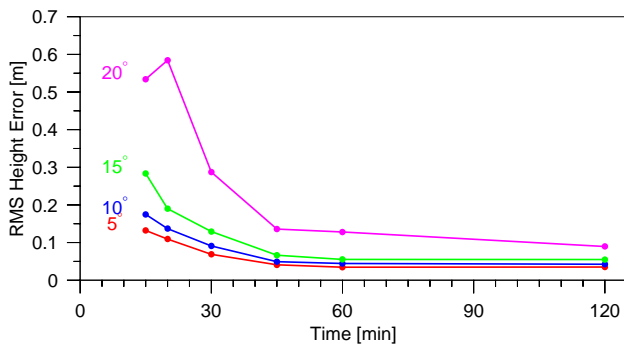


Fig. 11. RMS of height errors for varying batch lengths, with estimated residual tropospheric zenith delay and a constant weighting function.

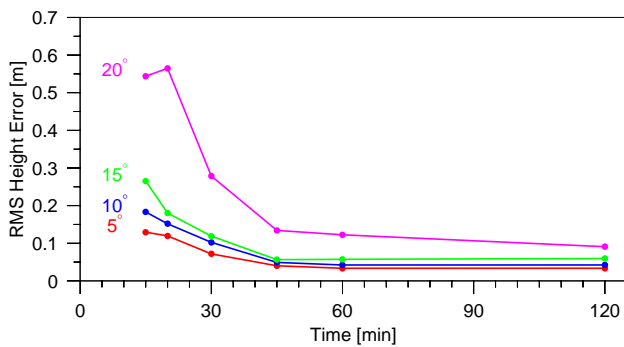


Fig. 12. RMS of height errors for varying batch lengths, with estimated residual tropospheric zenith delay and the standard weighting function.

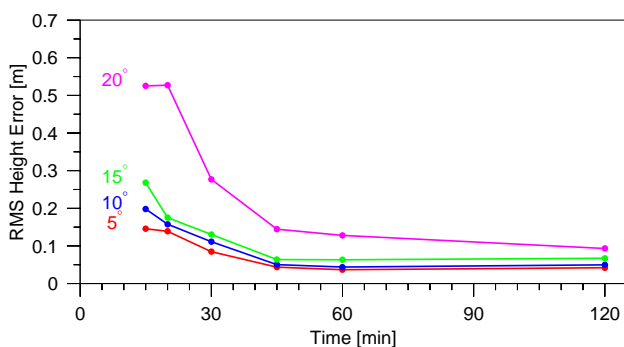


Fig. 13. RMS of height errors for varying batch lengths, with estimated residual tropospheric zenith delay and the reciprocal of sine as weighting function.

the processing. An overall feature in this data set is that the gain achieved by the zenith delay parameter is superior to the loss of geometric strength due to the extra parameter. Even for batches as short as a few tens of minutes the estimation of residual tropospheric zenith delay appears to be advantageous. When depending on the a priori model only, there is a very small gain in accuracy when increasing the time-span further than approximately 1 hour.

In the case of estimating zenith delay parameters, the use of low elevation data is beneficial while in the case of depending on the a priori model only, the low elevation data introduces a bias into the solution. As depicted in Figure 5, there is a significant gain in geometric information when lowering the elevation cut-off angle.

When using the a priori model only, the use of reciprocal sine of elevation as weighting function is beneficial. As seen in Figure 1, low elevation data is effectively down-weighted using the reciprocal sine of elevation. In the case of estimating zenith delay parameter, the differences between using weighting function are small but the use of the standard model appears to give the best results.

## SUMMARY AND CONCLUSION

From 40 days of marine test-data, an arbitrary set of 12 hours has been analyzed. Based on this data, it appears that the estimation of residual tropospheric zenith delay parameters is beneficial for observation scenarios as short as a few minutes.

In the case of estimating zenith delay parameters, the inclusion of low elevation data consistently improves the results. Using a state-of-the-art PPP software for kinematic processing, height coordinates at the sub-decimeter level is reached after approximately 30 minutes at the one sigma level and after 60 minutes at the 2 sigma level.

## ACKNOWLEDGMENTS

The authors would like to thank the Norwegian Hydrographic Service for providing the test data and reference trajectory.

We greatly acknowledge the efforts made by the IGS to deliver high quality data and products.

## REFERENCES

- Beutler, G., Rothacher, M., Schaer, S., Springer, T., Kouba, J. and Neilan, R. (1999). The International GPS Service (IGS): An Interdisciplinary Service in Support of Earth Sciences. *Advances in Space Research*, **23**(4), pp. 631–635.
- Collins, J. P. and Langley, R. B. (1997). *A Tropospheric Delay Model for the User of the Wide Area Augmentation System*. Technical Report 187, The Geodetic Research Laboratory, Department of Geomatics Engineering, University of New Brunswick, Canada.
- Collins, J. P. and Langley, R. B. (1998). The Residual Tropospheric Propagation Delay: How Bad Can It Get? In

- Proceedings of ION GPS 1998*, pp. 729–738, Nashville, TN.
- Gelb, A. (editor) (1974). *Applied Optimal Estimation*. The M.I.T. Press. ISBN 0262570483.
- Hopfield, H. S. (1971). Tropospheric effect on electromagnetically measured range: Prediction from surface weather data. *Radio Science*, **6**(3), pp. 357–367.
- ICD-GPS-200c (2000). *Navstar GPS Space Segment / Navigation User Interfaces (ICD-GPS-200c-004)*. Arinc Research Corporation, El Segundo, CA, USA.
- Jensen, A. B. O. and Øvstedal, O. (2006). Tropospheric Models in Precise Point Positioning. *Survey Review*. Accepted for publication.
- Kouba, J. and Heroux, P. (2001). GPS Precise Point Positioning Using IGS Orbit Products. *GPS Solutions*, **5**(2), pp. 12–28.
- Kristiansen, O. and Harrson, B. G. (1996). Nytt geodetisk grunnlag EUREF89. GPS kampanjen 1994 og analysere-sultater, EUREF89-NOR94. *Kart og plan*, (2), pp. 104–115. In Norwegian.
- Mader, G. L. (1999). GPS Antenna Calibration at the National Geodetic Survey. *GPS Solutions*, **3**(1), pp. 50–58.
- McCarthy, D. D. and Pétit, G. (editors) (2004). *IERS Conventions (2003)*. Verlag des Bundesamtes für Kartographie und Geodäsie, Frankfurt am Main. IERS Technical Note No. 32.
- Niell, A. E. (1996). Global mapping functions for the atmosphere delay at radio wavelengths. *Journal of Geophysical Research*, **101**(B2), pp. 3227–3246.
- Saastamoinen, J. (1973). Contributions to the theory of atmospheric refraction. *Bulletin Géodésique*, **107**(1), pp. 13–34. Part 3 of 3.